Materials Chemistry and Physics 188 (2017) 125–130

Contents lists available at ScienceDirect

Materials Chemistry and Physics

journal homepage: www.elsevier.com/locate/matchemphys

Kinetics of bainite precipitation in the $Cu_{69.3}Al_{18.8}Mn_{10.3}Ag_{1.6}$ alloy

M.B.J.L. Motta [a], A.T. Adorno [b], C.M.A. Santos [b], R.A.G. Silva [a, *]

[a] Departamento de Ciências Exatas e da Terra, UNIFESP, Diadema, SP, Brazil
[b] Departamento de Físico-Química, IQ-UNESP, Araraquara, SP, Brazil

HIGHLIGHTS

- The activation energy for the bainite precipitation in the $Cu_{69.3}Al_{18.8}Mn_{10.3}Ag_{1.6}$ alloy is around 33 kJ/mol.
- During bainite precipitation the Cu_2AlMn phase formation occurs.
- The $Cu_3Al(DO_3) \rightarrow Cu_2AlMn(L2_1)$ ordering reaction interferes in the activation energy value.

GRAPHICAL ABSTRACT

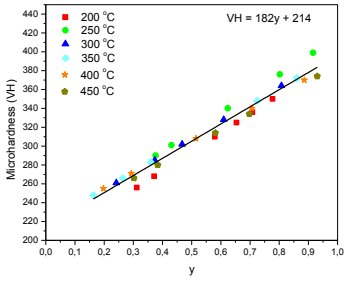

ARTICLE INFO

Article history:
Received 20 June 2016
Received in revised form
19 September 2016
Accepted 11 December 2016
Available online 21 December 2016

Keywords:
Metals and alloys
Aging
Kinetics

ABSTRACT

In this work the kinetics of bainite precipitation in the $Cu_{69.3}Al_{18.8}Mn_{10.3}Ag_{1.6}$ alloy was studied using measurements of microhardness change with aging time, scanning electron microscopy (SEM), energy dispersive X-ray (EDX) analyses, measurements of magnetization change with applied field and high-resolution transmission electron microscopy (HRTEM). The results showed that the bainite precipitation is responsible for the hardness increase in the $Cu_{69.3}Al_{18.8}Mn_{10.3}Ag_{1.6}$ alloy. The activation energy value obtained for the bainite precipitation is lower than that found in the literature. This was attributed to the presence of Ag dissolved in matrix and the occurrence of the $Cu_3Al(DO_3) \rightarrow Cu_2AlMn(L2_1)$ ordering reaction together with the bainite precipitation.

1. Introduction

The Cu-Al system is between the sets of most important alloys studied, since it presents almost all kinds of phase transformations described in literature. Besides that, Cu-Al alloys can have a great technologic importance related to light alloys for aeronautic industry in Al-rich corner, and the presence of the martensitic transformation in Cu-rich corner. The martensitic phase is associated with shape memory effect [1,2]. Normally these alloys are found as ternary and quaternary systems. The addition of other alloying elements to Cu-Al alloys is quite attractive and can modify different properties of these alloys [1,3–6]. The manganese addition introduces magnetic effects ascribed to the presence of the Cu_2AlMn phase [3,6], stabilizes the β phase [7–9] and produces Cu-Al-Mn alloys with shape memory effect and remarkable features [10]. The addition of silver to Cu-Al alloys is responsible for the increase in the martensitic transformation temperature [11], in hardness [12] and in corrosion resistance in these materials [13]. The silver also modifies the phase relations in Cu-Al alloys and can decrease the martensitic decomposition rate into $(\alpha+\gamma_1)$ in some compositions of Cu-Al-Ag alloys [12]. The Cu-Al-Ag and Cu-Al-Mn alloys are very sensitive to heat treatments and, therefore, the aging effects can promote interesting modifications in its microstructures. In this work the kinetics of bainite precipitation in the

* Corresponding author.
E-mail address: galdino.ricardo@gmail.com (R.A.G. Silva).

http://dx.doi.org/10.1016/j.matchemphys.2016.12.019
0254-0584/

$Cu_{69.3}Al_{18.8}Mn_{10.3}Ag_{1.6}$ alloy was studied to evaluate the extension of Mn and Ag contributions for the microstructure and microhardness changes in the quaternary alloy.

2. Experimental procedure

The $Cu_{69.3}Al_{18.8}Mn_{10.3}Ag_{1.6}$ alloy (at.%) was prepared in an arc furnace under argon atmosphere using 99.95% copper, 99.97% aluminum, 99.98% silver and 99.95% manganese as starting materials. Cylindrical samples of 10 mm diameter and 40 mm length were cut in disks of 2.0 mm thickness used for microhardness measurements and high-resolution transmission electron and scanning electron microscopies. These samples were annealed for 120 h at 850 °C for homogenization and after annealing they were maintained at 850 °C for 1 h and quenched in water at 0 °C. After the heat treatments the samples were polished and etched with a solution consisting of 10 g $FeCl_3.6H_2O_{(s)}$ + 25 mL $HCl_{(aq)}$ 36.5% to prepare 100 mL of aqueous solution. The Vickers microhardness measurements were made with a HMV-2T SHIMADZU TESTER using a load of 9.8 N for 30 s. Each hardness number was calculated from an average of 10 hardness impressions, with a standard deviation of about 2%. The measurements of microhardness changes with the aging time were made in samples quenched from 850 °C in water at 0 °C and then aged in the temperature range from 200 °C to 450 °C. Scanning electron micrographs (SEM) were obtained at different aging times to characterize the microstructures of the alloy. The scanning electron micrographs were obtained using a FEI-QUANTA 650 FEG High-resolution microscope with energy dispersive X-ray (EDX) analyses and High-resolution transmission electron micrographs (HRTEM) were obtained using a Philips microscope, model CM200, operating at 200 kV. The magnetization measurements with applied field were made using a PPMS 9 Evercool Quantum Design with samples aged at 400 °C for different times, mass at about ~2 mg and magnetic field from 0 to 50 kOe at 25 °C.

3. Results and discussion

Fig. 1(a–b) shows the plots of microhardness changes with aging time obtained for the $Cu_{69.3}Al_{18.8}Mn_{10.3}Ag_{1.6}$ alloy aged at 200 °C and 400 °C. The starting points of these curves correspond to samples quenched from 850 °C in water at 0 °C. From Fig. 1(a–b) and similar curves obtained at 250, 300, 350 and 450 °C it is possible to observe an incubation period, which decreases with the temperature increase and a hardness maximum for all temperatures. This hardness peak is shifted to lower aging times with the increase of temperature and at temperatures higher than 350 °C a hardness decrease is observed for higher aging times, and the microhardness reaches values close to those verified at the initial stages of aging.

Fig. 2 shows the scanning electron micrographs (SEM) obtained for the alloy aged at 400 °C for different aging times. In these SEM images it is possible to see the lamellae formation, which become thicker with the increase of aging time. According to the literature [7] these lamellae correspond to the bainite phase. Plots of microhardness changes with aging time obtained at 400 °C (Fig. 1-b) and the SEM image shown in Fig. 2-c indicate that the bainite lamellae thickening is responsible for the hardness decrease at higher aging times. Moreover, Cu-rich nanoprecipitates were observed among the bainite lamellae after longer aging times, as seen in Fig. 2-d. These precipitates show an Ag content higher than that observed in the metallic matrix, as indicated in Fig. 3-a. No precipitate of the Ag-rich phase was observed by SEM, suggesting that the remaining silver is dissolved into the matrix. Fig. 3-b shows the plots of magnetization as function of the applied field obtained at 25 °C for samples aged at 400 °C at different times. In these curves it is possible to see that the saturation magnetization of the alloy is increased up to 5400 s, and then decreased up to 60000 s. This shows that the ferromagnetic Cu_2AlMn phase is produced up to 5400 s and then it is partially decomposed up to 60000 s. Therefore, the bainite precipitation occurs together with the formation of the ferromagnetic Cu_2AlMn phase. The Cu_2AlMn phase decomposition can lead to formation of the stable phases: T_3-Cu_3Al_2Mn, β_{Mn} and α. Fig. 4 shows the selected area diffraction pattern and high-resolution transmission microcopy (HRTEM) image obtained for a sample aged at 400 °C for 60000 s. These results confirm the presence of the β_{Mn} phase after longer aging times.

Fig. 5-a shows the plots of the transformed fraction as a function of the aging time obtained from microhardness curves with time. Considering that the bainite precipitation shows nucleation and growth after an incubation period and that there is a linear relationship between transformed fraction and microhardness increase (see Fig. 5-b), the kinetic process of bainite precipitation may be described by the Johnson-Mehl-Avrami-Kolmogorov (JMAK) equation [7],

$$y = 1 - \exp\left[-(kt)^n\right] \quad (1)$$

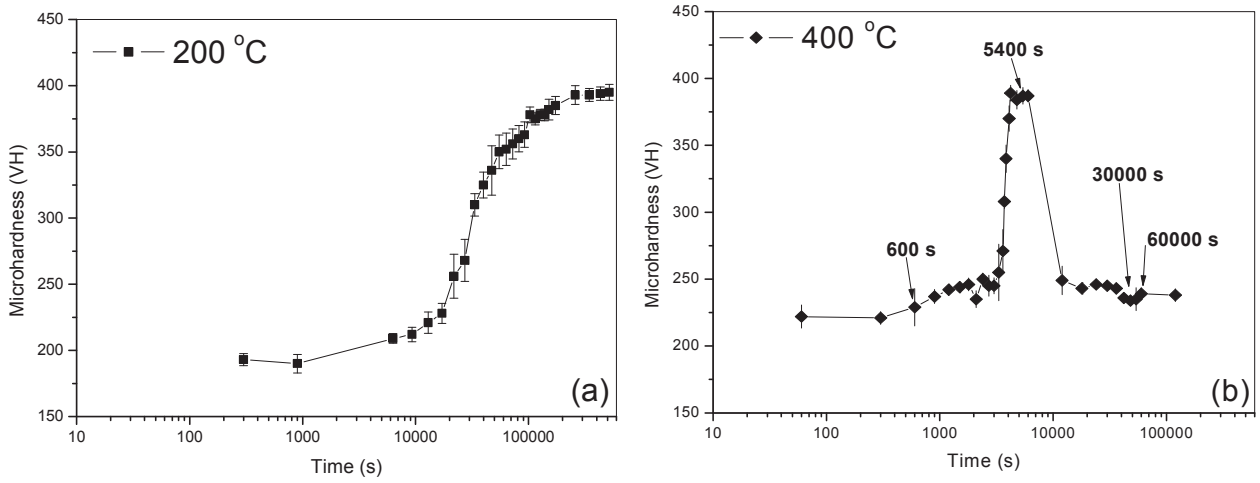

Fig. 1. Microhardness change curves with aging time obtained at 200 °C and 400 °C.

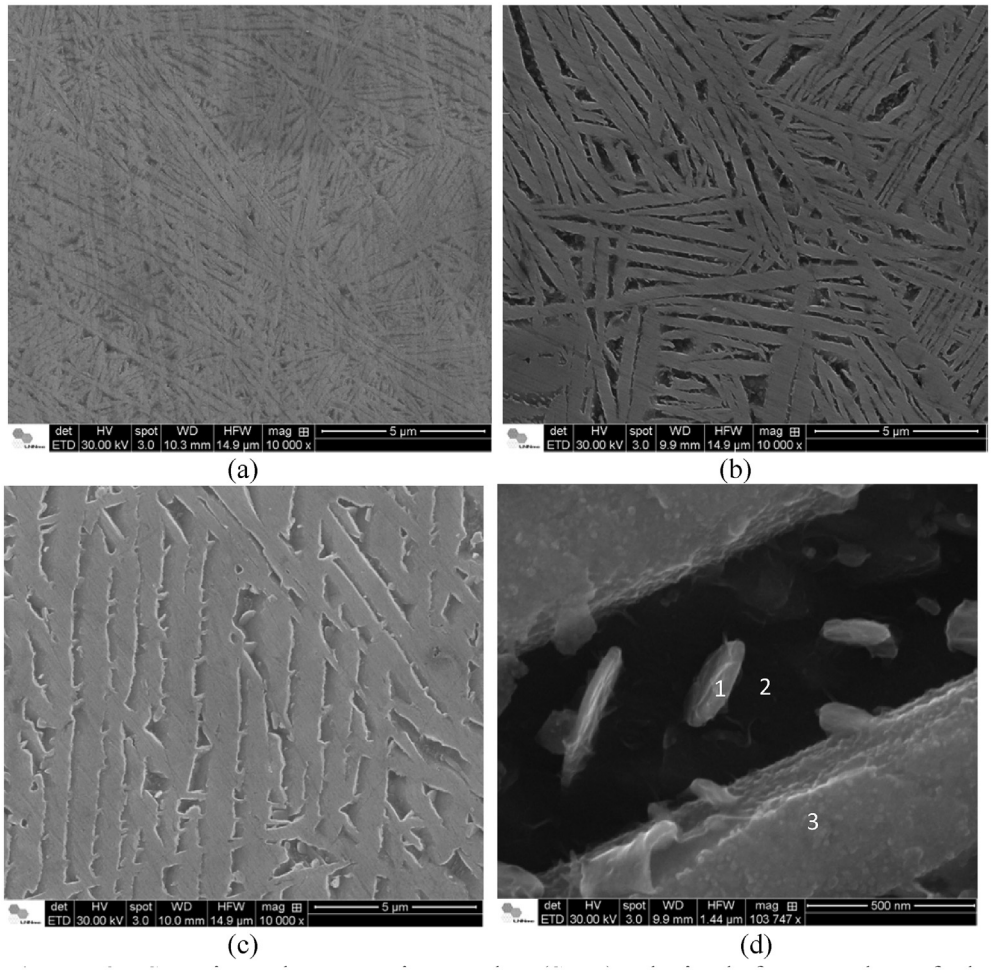

Fig. 2. Scanning electron micrographs (SEM) obtained for samples of the $Cu_{69.3}Al_{18.8}Mn_{10.3}Ag_{1.6}$ alloy aged at 400 °C for (a) 600 s, (b) 5400 s and (c) 60000 s. (d) Precipitates formed after aging at 400 °C for 30000 s.

which can be rewritten as

$$\ln[-\ln(1-y)] = n\ln k + n\ln t, \quad (2)$$

where y is the fraction of the product phase, k is the temperature-dependent rate constant, t is the time, n is the time exponent parameter depending on the nucleation mechanism.

The fit of equation (2) to the linear portion of the plot shown in

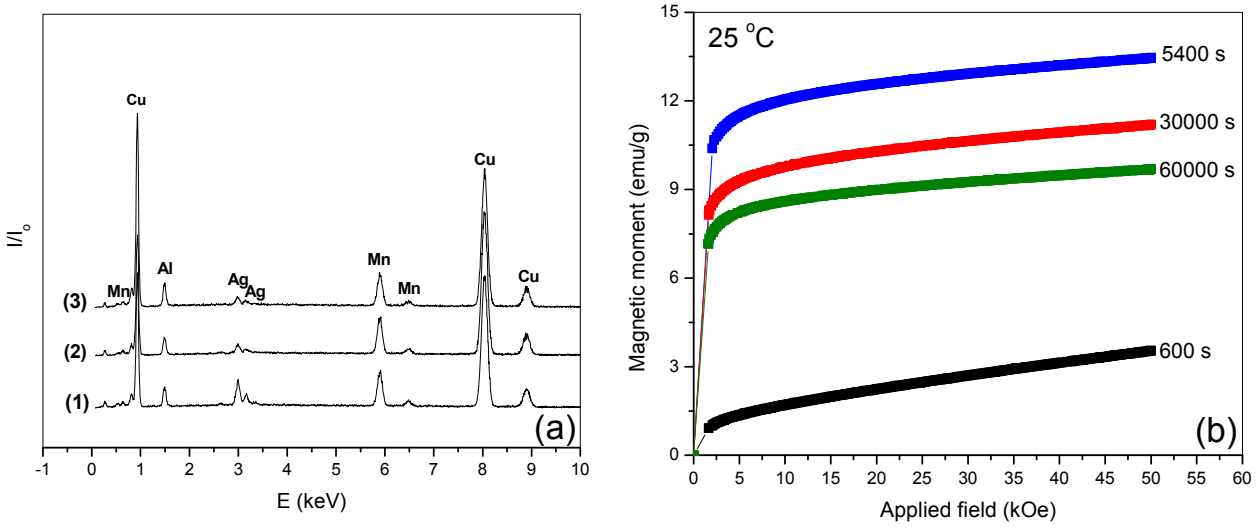

Fig. 3. (a) EDX spectrum obtained at regions defined in Fig. 2-d. (b) Curves of magnetization as function of the applied field obtained for samples aged at 400 °C in different aging times.

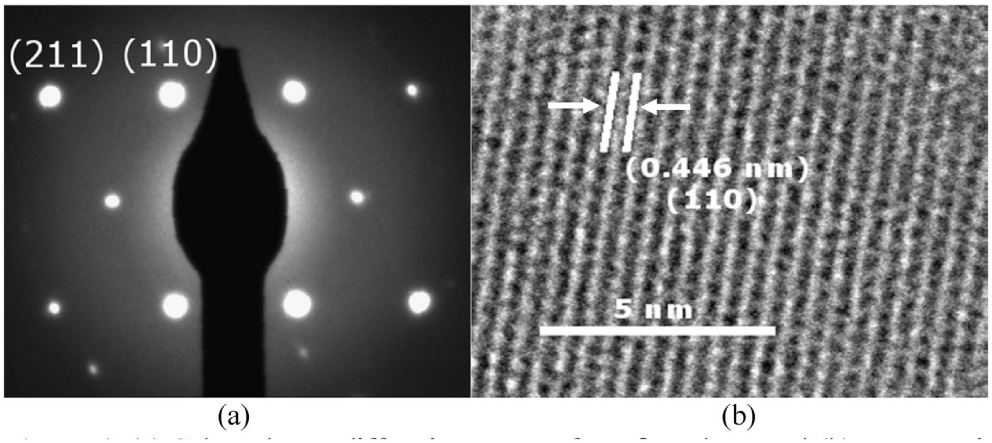

Fig. 4. (a) Selected area diffraction pattern from β_{Mn} phase and (b) HRTEM image showing details from β_{Mn} phase.

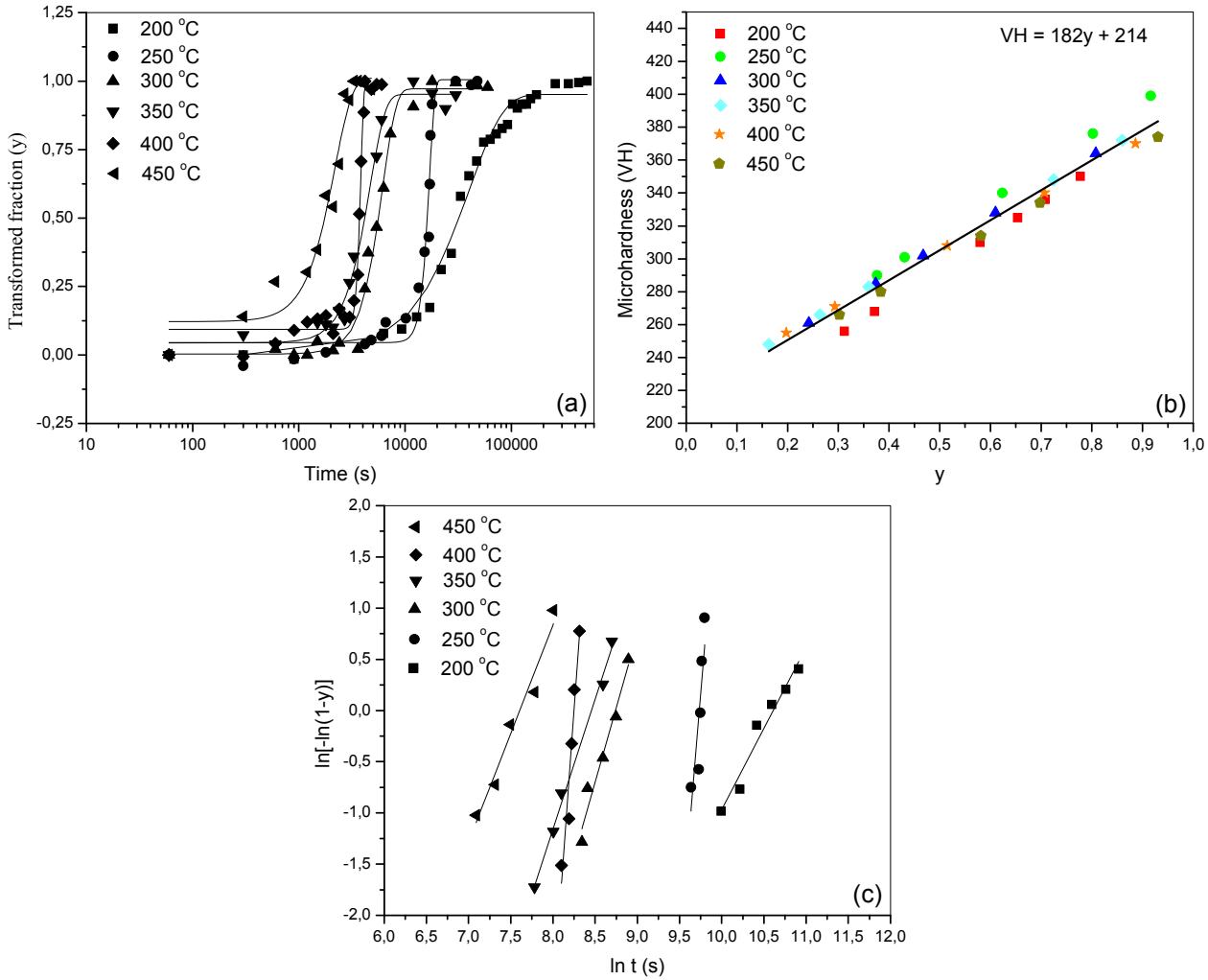

Fig. 5. (a) Transformed fraction changes with aging time. (b) Plot of microhardness with transformed fraction. (c) Plot of ln[−ln(1 − y)] vs. ln t.

Fig. 5-a provides straight lines with slope and linear coefficients related to the kinetic parameters of the bainite precipitation in the $Cu_{69.3}Al_{18.8}Mn_{10.3}Ag_{1.6}$ alloy.

Table 1 shows the values of n and k obtained from Fig. 5-c. The analysis of the n values obtained for the $Cu_{69.3}Al_{18.8}Mn_{10.3}Ag_{1.6}$ alloy indicates a diffusion controlled growth with all shapes growing from small dimensions: with zero nucleation rate ($n = 1½$) at 200 °C; increasing nucleation rate ($n > 2½$) at 250 and 300 °C; constant nucleation rate (n = 2½) at 350 °C; increasing nucleation rate ($n > 2½$) at 400 °C and decreasing nucleation rate ($n < 2½$) at

Table 1
Values of *n* and *k* obtained from Fig. 5-c.

Temperatures/°C	200		250		300		350		400		450	
Kinetic parameters	n	k/s^{-1}	n	k/s^{-1}	n	k/s^{-1}	n	k/s^{-1}	n	k/s^{-1}	n	k/s^{-1}
Values	1.50	2.47×10^{-5}	10.0	5.88×10^{-5}	2.90	1.60×10^{-4}	2.50	2.12×10^{-4}	11.4	2.61×10^{-4}	2.12	4.97×10^{-4}

450 °C [14].

These values of *n* suggest that at 200 °C the growth process of bainite lamellae did not have started, from 250 °C to 300 °C this phase growths and reaches a maximum at about 350 °C. From this stage the growth process is completed and the thickening step begins, as seen in Fig. 2. These results are according to literature data for the $Cu_{71}Al_{18}Mn_{11}$ alloy [8] that show an isochronal curve with maximum hardness at about 300 °C. At 400 °C there is a new increase in the nucleation rate, probably due to the diffusion of Ag to the Cu-rich precipitates, as seen in Fig. 2-d and Fig. 3-a. Precipitates of Ag can be formed at about 400 °C, as reported in the literature [15]. This effect is concluded at about 450 °C because of high temperature and the beginning of Ag dissolution, and then the nucleation rate decreases again at 450 °C.

Considering the Arrhenius equation,

$$k = k_o \exp(-E_a/RT), \quad (3)$$

where k_0 is the pre-exponential factor, E_a is the activation energy for the process, *T* is the absolute temperature and *R* is the gas constant, the *k* values shown in Table 1 can be used to estimate the activation energy for the bainite precipitation from the slope of the plot of ln *k vs. 1/T*, as seen in Fig. 6. For the $Cu_{69.3}Al_{18.8}Mn_{10.3}Ag_{1.6}$ alloy the activation energy was $E_a = (33.0 \pm 2.5)$ $kJmol^{-1}$. This value is lower than activation energies found in the literature for aged alloys in the same temperature range (see Table 2). The error associated with the activation energy value obtained in this work can be related to the presence of variable fractions of other phases together with the bainitic phase.

It is known [16] that in the $Cu_{81}Al_{19}$ alloy the aging in the temperature range from 200 to 600 °C promotes the ($\alpha+\gamma_1$) phase formation, while in the $Cu_{71.9}Al_{16.6}Mn_{9.3}Ni_2B_{0.2}$ alloy the presence of Mn stabilizes the β phase on quenching and during aging the ($\alpha+\gamma_1$) phase formation is suppressed, and only the bainite precipitation is detected [7]. In the $Cu_{78.7}Al_{19.2}Ag_{2.1}$ alloy the formation of Ag-rich precipitates occurs and a decrease in the ($\alpha+\gamma_1$) formation rate is observed. In this case, the formation of the Ag-rich phase is catalyzed by the presence of γ_1 [12].

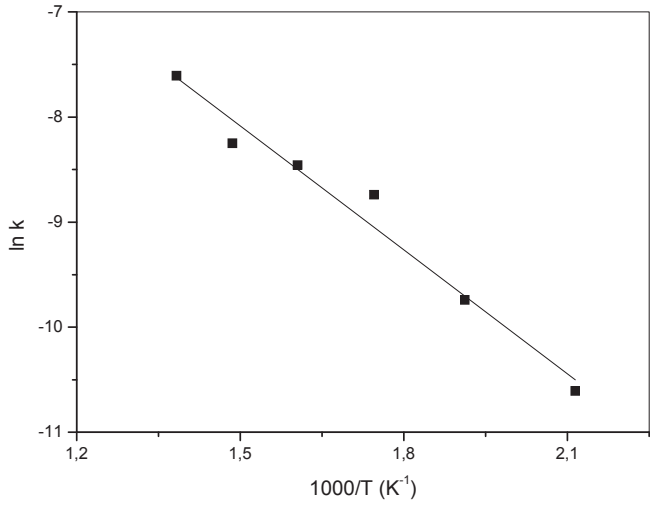

Fig. 6. Plot of ln *k* vs. 1/T.

Table 2
Activation energies for aged alloys in the same temperature range.

Alloys	Activation energies	References
$Cu_{69.3}Al_{18.8}Mn_{10.3}Ag_{1.6}$	33 kJ/mol	In this work
$Cu_{81}Al_{19}$	42 kJ/mol	[16]
$Cu_{78.7}Al_{19.2}Ag_{2.1}$	60 kJ/mol	[12]
$Cu_{71.9}Al_{16.6}Mn_{9.3}Ni_2B_{0.2}$	60 kJ/mol	[7]
$Cu_{67.7}Zn_{19.2}Al_{13.1}$	72 kJ/mol	[17]

In the $Cu_{69.3}Al_{18.8}Mn_{10.3}Ag_{1.6}$ alloy the precipitation of the Ag-rich phase was expected, but it was not observed by scanning electron microscopy. The bainite precipitation occurred before the Ag-rich phase precipitation and together with the Cu_2AlMn phase formation. Therefore, the matrix was saturated with silver atoms when the bainite precipitation occurred. The instability caused by the presence of silver into the matrix contributed for the decrease in the activation energy for the bainite precipitation, since this reaction decreases the Gibbs energy of the $Cu_{69.3}Al_{18.8}Mn_{10.3}Ag_{1.6}$alloy. Furthermore, $Cu_2AlMn(L2_1)$ phase formation is due to ordering of the $Cu_3Al(DO_3)$ phase, in which the Cu atoms in the DO_3 phase sublattice are substituted by Mn atoms [9]. Therefore, a higher amount of Cu atoms is available for the bainite formation when the $Cu_3Al(DO_3) \rightarrow Cu_2AlMn(L2_1)$ ordering reaction occurs. This can also contribute for the decrease in activation energy for the bainite precipitation in the $Cu_{69.3}Al_{18.8}Mn_{10.3}Ag_{1.6}$ alloy.

The γ_1 phase in Cu-Al alloys has a complex body-centered cubic structure with lattice parameter about three times that of a corresponding body-centered cubic metal [12,18]. This contributes for diffusion of Ag dissolved in the matrix on quenching and, consequently, for formation of Ag-rich precipitates during aging of the quenched $Cu_{78.7}Al_{19.2}Ag_{2.1}$ alloy [12]. When ~10 at%Mn was added to the Cu-Al-Ag alloy the eutectoid reaction was suppressed and the γ_1 phase was not produced. Considering that the Ag-Al and Ag-Mn interactions are stronger than the Cu-Ag interaction, the presence of Ag dissolved in the matrix can be decreasing the Mn and Al diffusion rates, without interfere significantly on Cu diffusion rate. This contributed for the precipitation of bainitic phase, which is richer in Cu, thus decreasing the activation energy for this reaction in the $Cu_{69.3}Al_{18.8}Mn_{10.3}Ag_{1.6}$ alloy. This can also explain the great difference between the activation energy values found for the $Cu_{78.7}Al_{19.2}Ag_{2.1}$ alloy (with formation of the γ_1 phase and with Ag precipitation) [12] and that obtained in this work (without formation of the γ_1 phase and without Ag precipitation).

4. Conclusions

The results showed that the bainite precipitation is responsible for the microhardness increase in the $Cu_{69.3}Al_{18.8}Mn_{10.3}Ag_{1.6}$ alloy. During bainite precipitation the Cu_2AlMn phase formation occurs. The bainite lamellae thickening decreases the alloy microhardness at higher aging times. The activation energy value obtained for bainite precipitation is lower than that found in the literature. This was attributed to the presence of Ag dissolved in the matrix and to

the $Cu_3Al(DO_3) \rightarrow Cu_2AlMn(L2_1)$ ordering reaction.

Acknowledgments

The authors thank to FAPESP (2011/11041-4) and CNPq (301759/2012-0) for financial support, and LNNano for technical support during electron microscopy work (FEI Quanta 650 FEG – High Resolution SEM).

References

[1] S. Yang, T. Omori, C. Wang, Y. Liu, M. Nagasako, J. Ruan, R. Kainuma, K. Ishida, X. Liu, A jumping shape memory alloy under heat, Sci. Rep. 6 (2016) 21754, http://dx.doi.org/10.1038/srep21754.
[2] J.M. Jani, M. Leary, A. Subic, M.A. Gibson, A review of shape memory alloy research, applications and opportunities, Mater. Des. 56 (2014) 1078–1113.
[3] R.A.G. Silva, A. Paganotti, S. Gama, A.T. Adorno, T.M. Carvalho, C.M.A. Santos, Investigation of thermal, mechanical and magnetic behaviors of the Cu-11%Al alloy with Ag and Mn additions, Mater. Charact. 75 (2013) 194–199.
[4] C.H. Chen, T.F. Liu, Phase transformations in a Cu-14.2Al-15.0Ni alloy, Mater. Chem. Phys. 78 (2002) 464–473.
[5] J. Lelatko, H. Morawiec, The effect of Ni, Co and Cr on the primary particle structure in Cu-Al-Nb-X shape memory alloys, Mater. Chem. Phys. 81 (2003) 472–475.
[6] S.Y. Yang, T.F. Liu, As-quenched microstructures of $Cu_{3-x}Mn_xAl$ alloys, Mater. Chem. Phys. 98 (2006) 389–394.
[7] Y. Sutou, N. Koeda, T. Omori, R. Kainuma, K. Ishida, Effects of ageing on bainitic and thermally induced martensitic transformations in ductile Cu-Al-Mn-based shape memory alloys, Acta Mater. 57 (2009) 5748–5758.
[8] Y. Sutou, T. Omori, A. Furukawa, Y. Takahashi, R. Kainuma, K. Yamauchi, S. Yamashita, K. Ishida, Development of medical guide wire of Cu-Al-Mn-Base superelastic alloy with functionally graded characteristics, J. Biomed. Mater. Res. Part B Appl. Biomater. 69B (2004) 64–69.
[9] R. Kainuma, N. Satoh, X.J. Liu, I. Ohnuma, K. Ishida, Phase equilibria and Heusler phase stability in the Cu-rich portion of the Cu-Al-Mn system, J. Alloys Compd. 266 (1998) 191–200.
[10] R. Kainuma, S. Takahashi, K. Ishida, Thermoelastic martensite and shape memory effect in ductile, Metallurg. Mater. Trans. A 27A (1996) 2187–2195.
[11] J.M. Guilemany, J. Fernández, R. Franch, A.V. Benedetti, A.T. Adorno, A new Cu-Based SMA with extremely high martensitic transformation temperatures, J. Phys. IV Fr. 05 (1995). C2-361–C2-365.
[12] A.T. Adorno, R.A.G. Silva, Isothermal decomposition kinetics in the Cu-9%Al-4% Ag alloy, J. Alloys Compd. 375 (2004) 128–133.
[13] A.V. Benedetti, P.T.A. Sumodjo, K. Nobe, P.L. Cabot, W.G. Proud, Electrochemical studies of copper, copper-aluminium and copper-aluminium-silver alloys: impedance results in 0.5M NaCl, Electrochim. Acta 40 (16) (November 1995) 2657–2668.
[14] J.W. Christian, The Theory of Transformations in Metals and Alloys Part 1, third ed., Pergamon Press, Oxford, 2002.
[15] A.T. Adorno, R.A.G. Silva, Reverse martensitic transformation in the Cu-10 wt% Al-6 wt%Ag alloy, J. Mater. Sci. 40 (2005) 6217–6221.
[16] A.T. Adorno, M.R. Guerreiro, A.V. Benedetti, Isothermal aging kinetics in the Cu-19 at.%Al alloy, J. Alloys Compd. 315 (2001) 150–157.
[17] N.F. Kennon, D.P. Dunne, L. Middleton, Aging effects in copper-based shape memory alloys, Metall. Trans. 13A (1982) 551–555.
[18] R.E. Smallman, W. Hume-Rothery, W. Haworth, The Structure of Metals and Alloys, The Institute of Metals, London, 1988.